

ASSESSMENT OF MULTIFRAGMENTATION UNDER THE EFFECT OF SYMMETRY ENERGY

*Rubina Bansal, Suneel Kumar*¹

School of Physics and Materials Science, Thapar University, Patiala, Punjab, India

We study the effect of symmetry energy on the fragment production for the reactions ${}^{20}_{10}\text{Ne}_{10} + {}^{20}_{10}\text{Ne}_{10}$ and ${}^{197}_{79}\text{Au}_{118} + {}^{197}_{79}\text{Au}_{118}$ for the incident energy range of 50–1000 MeV/nucleon using isospin-dependent quantum molecular dynamics (IQMD) model. Our study shows that the density-dependent symmetry energy plays a significant role in multiplicity of fragments produced at low energy. Moreover, sensitivity of density-dependent symmetry energy decreases with increase in neutron content of colliding system. We also compare the symmetry energy suggested by different groups. A comparative study of experimental results with theoretical calculations of IQMD shows that the density-dependent symmetry energy is a good probe to explain the multiplicity of the fragments at low energy.

Изучается влияние эффекта симметрии энергии на фрагментацию ядер в реакциях ${}^{20}_{10}\text{Ne}_{10} + {}^{20}_{10}\text{Ne}_{10}$ и ${}^{197}_{79}\text{Au}_{118} + {}^{197}_{79}\text{Au}_{118}$ в интервале начальных энергий 50–1000 МэВ/нуклон с помощью зависящей от спина модели квантовой молекулярной динамики. Проведенное исследование показывает, что зависящая от плотности симметрия энергии играет важную роль в определении множественности фрагментов, образующихся при низких энергиях. Кроме того, показано, что чувствительность к данному эффекту падает с увеличением содержания нейтронов в сталкивающейся системе. Полученные результаты сравниваются с результатами других групп. Из сравнения с экспериментальными данными видно, что зависящая от плотности симметрия энергии является хорошим инструментом для объяснения множественности фрагментов реакции столкновения ядер при низких энергиях.

PACS: 25.70.-z; 25.75.Ld

INTRODUCTION

The science of nuclear physics deals with the properties of nuclear matter. The study of nuclear matter and strength of nuclear interaction is a key to understand many fundamental problems. The understanding of the behavior of nuclear matter at density away from normal nuclear matter ($T \approx 0$ MeV, $\rho_0 \approx 0.17$ fm⁻³) has gained tremendous importance [1]. In the past decades, only light ions or particles could be accelerated to produce the collisions. But now it is possible to accelerate the heavy-ion beams of high energy. The term heavy ion is generally used for the nuclei which are heavier than the helium nucleus. The heavy-ion collisions have attracted the scientific world because of their various features, e.g., these are helpful in studying the nuclear matter at extreme conditions of temperature and pressure, which can be correlated with astrophysical happening like supernova explosion, neutron star, etc.

¹E-mail: suneel.kumar@thapar.edu

Multifragmentation is one of the important phenomena occurring at intermediate energies. The process of breaking of colliding nuclei into several small, medium-size fragments is called multifragmentation. Highly excited and neutron-rich fragments subsequently undergo deexcitation to cold and stable isotopes. The parameters that effect the multifragmentation are impact parameter, incident energy, equation of state, and cross section. Symmetry energy ($E_{\text{sym}}(\rho)$) can effect the multifragmentation due to the collision between two nuclei. $E_{\text{sym}}(\rho)$ of nuclear matter characterizes the energy changes, as one moves away from symmetric to asymmetric systems. So, it is an interesting and important goal of heavy-ion physics to extract information about symmetry energy and its density dependence. Many microscopic and/or phenomenological many-body theories using various interactions [2, 3] predicted that the symmetry energy increases continuously at all densities. However, other models [4–6] predicted that the symmetry energy first increases to a maximum and then may start decreasing at certain supra-saturation densities. Many groups have estimated the different values of E_{sym} [7–9] to see the influence of compressibility through symmetry energy.

In multifragmentation, the measurement of fragment isotopic yield distribution can provide important insight into the symmetry energy and the decay characteristics of the nuclei. So far, the isoscaling behavior has been studied experimentally and theoretically for different reaction mechanisms [10–12]. D. V. Shetty et al. [13, 14] experimentally understood the correlation between the temperature, density and symmetry energy of multifragmenting system as it evolves with excitation energy. They also studied the relative reduced neutron and proton densities as a function of excitation energy of fragmenting source for the ${}^{58}_{26}\text{Fe}_{32} + {}^{58}_{28}\text{Ni}_{30}$ and ${}^{58}_{26}\text{Fe}_{32} + {}^{58}_{26}\text{Fe}_{32}$ reactions. Their study reveals that there is a steady decrease in neutron density and an increase in proton density for an increase in the excitation energy.

But still no comparative study on the effect of density-dependent symmetry energy (DDSE) at low and high energy exist. In this paper we compare the various forms of symmetry energy suggested by different groups with our suggested values of symmetry energy and tried to understand the influence of DDSE on multiplicity of fragments (where $\rho = 0.1\text{--}0.3\rho_0$ away from normal nuclear matter density) for neutron-rich and neutron-deficient nuclei at different incident energies as well as impact parameters. To verify the results, we compare our theoretical results with experimental data [15]. This study is done within the framework of the isospin-dependent quantum molecular dynamics model [16, 17]. Section 1 deals with the model, Sec. 2 discusses the symmetry energy and characteristics of the results.

1. ISOSPIN-DEPENDENT QUANTUM MOLECULAR DYNAMICS (IQMD) MODEL

Our study is performed within the framework of the IQMD [16] model. This model is an improved version of the QMD model [18–21] developed by J. Aichelin and co-workers. The model has been applied successfully to extract the information about various phenomena such as collective flow, disappearance of flow [22–24] and fragmentation [25–28]. The isospin degree of freedom enters into the calculations through symmetry potential and cross section [16, 17]. This model includes three important steps: First, one has to generate the nuclei. This procedure is called initialization. The successfully generated nuclei propagate under the influence of surrounding mean field. This is termed propagation. Finally, nucleons are bound to collide if they come too close to each other. This part is dubbed as collisions. The details about the elastic and inelastic cross sections for proton–proton and neutron–neutron

collisions can be found in [16,17]. In the IQMD model, the nucleons of target and projectile interact via two- or three-body Skyrme forces, Yukawa potential and Coulomb interactions. In addition to the use of explicit charge states of all baryons and mesons, a symmetry potential between protons and neutrons corresponding to the Bethe–Weizsäcker mass formula has been included. This helps in achieving correct distribution of protons and neutrons within the nucleus. Skyrme forces are successful in the analysis of low-energy phenomena such as fusion, fission and cluster-radioactivity, where nuclear potential plays an important role [29].

The hadrons propagate using classical Hamilton equations of motion:

$$\frac{dr_i}{dt} = \frac{d\langle H \rangle}{dp_i}, \quad \frac{dp_i}{dt} = -\frac{d\langle H \rangle}{dr_i}, \quad (1)$$

with

$$\begin{aligned} V^{ij}(\mathbf{r}' - \mathbf{r}) &= V_{\text{Skyrme}}^{ij} + V_{\text{Yukawa}}^{ij} + V_{\text{Coul}}^{ij} + V_{\text{mdi}}^{ij} + V_{\text{sym}}^{ij} = \\ &= \left[t_1 \delta(\mathbf{r}' - \mathbf{r}) + t_2 \delta(\mathbf{r}' - \mathbf{r}) \rho^{\gamma-1} \left(\frac{\mathbf{r}' + \mathbf{r}}{2} \right) \right] + t_3 \frac{\exp(-|\mathbf{r}' - \mathbf{r}|/\mu)}{(|\mathbf{r}' - \mathbf{r}|/\mu)} + \frac{Z_i Z_j e^2}{|\mathbf{r}' - \mathbf{r}|} + \\ &\quad + t_4 \ln^2 (t_5 (p_i - p_j)^2 + 1) \delta(\mathbf{r}'_i - \mathbf{r}_j) + E_{\text{sym}}^0 \left(\frac{\rho}{\rho_0} \right)^\gamma. \end{aligned} \quad (2)$$

Here t_1 and t_2 are two- and three-body interactions, respectively, and t_3, t_4 and t_5 having values -6.66 , 1.5 MeV and $5 \cdot 10^{-4}$ MeV $^{-2}$, respectively. Here Z_i and Z_j denote the charges of i th and j th baryon, while $E_{\text{sym}}^0 = 32$ MeV for normal nuclear density ρ_0 , ρ is instantaneous density, γ is the stiffness parameter. The value of meson potential consists of Coulomb interaction only. The binary nucleon–nucleon collisions are included by employing the collision term of well-known VUU–BUU equation. During the propagation, two nucleons are supposed to suffer a binary collision if the distance between their centroids

$$|r_i - r_j| \leq \sqrt{\frac{\sigma_{\text{tot}}}{\pi}}, \quad \sigma_{\text{tot}} = \sigma(\sqrt{s}, \text{type}), \quad (3)$$

where σ_{tot} represents the total nucleon–nucleon (NN) cross section, \sqrt{s} is the center-of-mass energy and type denotes the ingoing collision partners ($N-N$, $N-\Delta$, $N-\pi, \dots$). In addition, Pauli blocking (of the final state) of baryons is taken into account by checking the phase space densities in the final states. The phase space generated using the IQMD model has been analyzed using the minimum spanning tree (MST) algorithm [29,30].

2. RESULTS AND DISCUSSION

We have simulated the symmetric reactions ${}^{20}_{10}\text{Ne}_{10} + {}^{20}_{10}\text{Ne}_{10}$ and ${}^{197}_{79}\text{Au}_{118} + {}^{197}_{79}\text{Au}_{118}$ at incident energies of 50, 100, 200, 400, 600, 1000 MeV/nucleon for central collision (scaled impact parameter $\hat{b} = 0.3$) using soft equation of state. For all calculations we take symmetry (E_{sym}^0) energy corresponding to the normal nuclear matter density is 32 MeV and value of γ which characterizes the stiffness of symmetry energy is 0, 0.66 and 2. In Fig. 1, we have displayed the parameterized values of density-dependent symmetry energy (DDSE) suggested by the various experimental and theoretical groups [7–9,31–37].

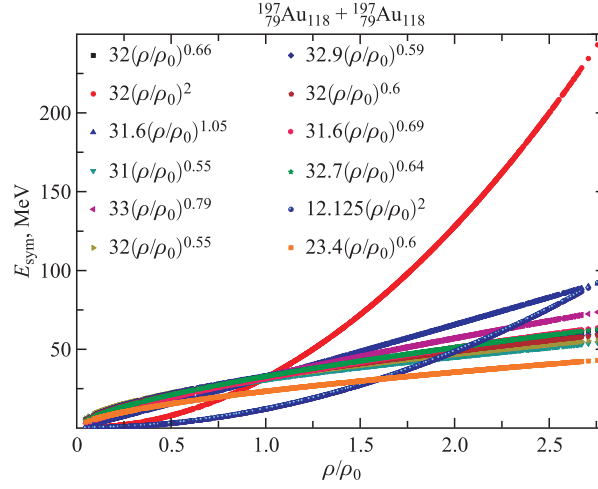


Fig. 1. Schematic diagram to show the density dependence of symmetry energy suggested by various groups

Two different types of the density-dependent forms of symmetry energy have been observed. One, where the symmetry energy increases monotonically with increasing density ("stiff" dependence) and the other, where the symmetry energy increases initially up to normal nuclear density and then decreases at higher densities ("soft" dependence). The stiffness increases by increasing the value of γ . The DDSE with $\gamma = 2$ is highly stiffer than others. One can clearly see in Fig. 1 that the DDSE is also influenced by E_{sym}^0 . The DDSE increases with increase in E_{sym}^0 . Generally, multifragmentation takes place at $\rho/\rho_0 = 0.1-0.3$, where $\rho_0 = 0.17 \text{ fm}^{-3}$ is normal nuclear matter density. In Fig. 1, one can clearly see the influence of DDSE in this range. To study the influence of both types of DDSE, we use $\gamma = 0.66$ (soft) and 2 (stiff) w.r.t $\gamma = 0$ (symmetry energy independent of density dependence).

In Fig. 2, we study the influence of DDSE on multiplicity at different incident energies (50–1000 MeV/nucleon). On the basis of mass, the fragments are classified as free nucleons (FNs) ($A = 1$), light mass fragments (LMFs) ($2 \leq A \leq 4$) and intermediate mass fragments (IMFs) ($5 \leq A \leq A_{\text{tot}}/(n)$, where $n = 6(3)$ for $^{197}\text{Au}_{118} + ^{197}\text{Au}_{118}$ ($^{20}\text{Ne}_{10} + ^{20}\text{Ne}_{10}$)). We observed that:

- (i) The fragment multiplicity is found to be sensitive to the strength of symmetry energy.
- (ii) The role of DDSE decreases with increase in incident energy. This happens because at higher incident energies the effect of symmetry energy is negligible and the whole reaction dynamics is governed by the NN collisions only.
- (iii) The DDSE is more sensitive in neutron-rich nuclei as compared to neutron-deficient nuclei for large γ value at low energy, because the symmetry potential for the neutron-rich systems is stronger compared to the neutron-deficient systems due to large relative neutron strength. Moreover, symmetry potential is attractive for protons and repulsive for neutrons.

To study the effect of DDSE on multiplicity in a more interesting way, we calculate the relative percentage ratio of fragment multiplicity for $\gamma = 0.66$ (soft) and 2 (stiff) w.r.t $\gamma = 0$ (symmetry energy independent of density dependence). The relative percentage ratio is calculated as

$$\text{Rel} [\%] = \left| \frac{\text{Mul}_{\gamma=0.66 \text{ or } 2} - \text{Mul}_{\gamma=0}}{\text{Mul}_{\gamma=0}} \right| \cdot 100. \quad (4)$$

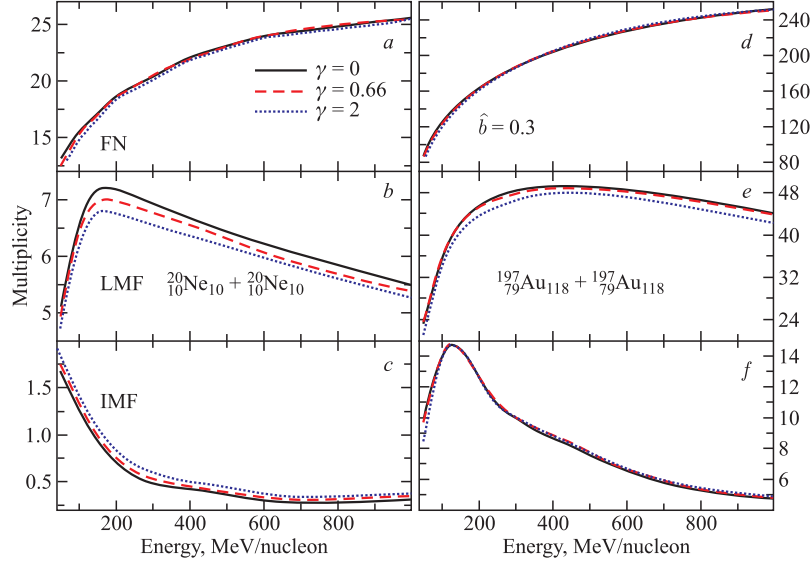


Fig. 2. Incident energy dependence of multiplicity of FNs, LMFs and IMFs for symmetric reactions of $^{197}_{79}\text{Au}_{118} + ^{197}_{79}\text{Au}_{118}$ and $^{20}_{10}\text{Ne}_{10} + ^{20}_{10}\text{Ne}_{10}$ at different incident energies for semi-central collision ($\hat{b} = 0.3$) for three different values of γ (0, 0.66, 2)

In Tables 1 and 2 we estimate the relative percentage ratio of FNs, LMFs and IMFs for $\gamma = 0.66$ and 2 w.r.t $\gamma = 0$ at incident energies of 50 and 1000 MeV/nucleon. Moreover, the relative percentage change in fragments multiplicity decreases as we go from $E = 50$ to 1000 MeV/nucleon. It has also been observed experimentally that a small change in multiplicity takes place beyond 400 MeV/nucleon [38]. Moreover, due to the large compression the relative percentage ratio of fragment multiplicity is large for $\gamma = 2$ as compared to the $\gamma = 0.66$ in all cases. So, one can conclude that the DDSE plays a significant role in fragment multiplicity (FNs and LMFs) at low energy; moreover, it is independent of DDSE at high energy.

Table 1. Relative production of FNs, LMFs and IMFs for DDSE with $\gamma = 0.66, 2$ w.r.t $\gamma = 0$ for the colliding system of $^{20}_{10}\text{Ne}_{10} + ^{20}_{10}\text{Ne}_{10}$ at incident energies of 50 and 1000 MeV/nucleon

Incident energy	Relative yield					
	FN		LMF		IMF	
γ	0.66	2	0.66	2	0.66	2
$E = 50$ MeV/nucleon	4	8.74	2.5	7.07	4.4	9.97
$E = 1000$ MeV/nucleon	0.38	0.81	2.04	3.94	13.65	25.07

Table 2. Same as Table 1 but for the colliding system of $^{197}_{79}\text{Au}_{118} + ^{197}_{79}\text{Au}_{118}$

Incident energy	Relative yield					
	FN		LMF		IMF	
γ	0.66	2	0.66	2	0.66	2
$E = 50$ MeV/nucleon	0.81	8.1	0.95	9.81	1	13.7
$E = 1000$ MeV/nucleon	0.21	0.4	0.31	4.14	1.33	4.027

Now to understand the effect of DDSE on the colliding geometry, in Figs.3 and 4, we display the multiplicity of fragments as a function of scaled impact parameter (b/b_{\max}). In both the figures, the panels *a* & *d*, *b* & *e* and *c* & *f* represent FNs, LMFs and IMFs, respectively. Left panels are for $^{20}_{10}\text{Ne}_{10} + ^{20}_{10}\text{Ne}_{10}$ and right panels for $^{197}_{79}\text{Au}_{118} + ^{197}_{79}\text{Au}_{118}$.

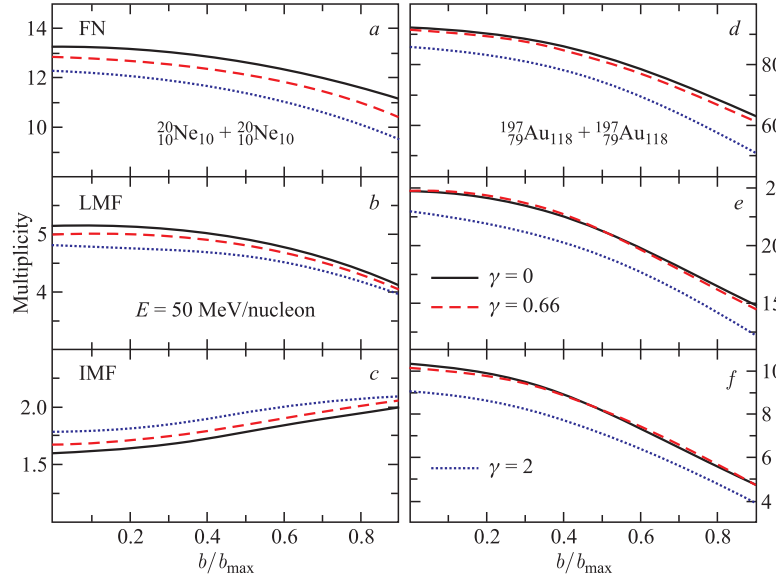


Fig. 3. Fragment multiplicity as a function of impact parameter for $^{20}_{10}\text{Ne}_{10} + ^{20}_{10}\text{Ne}_{10}$ (left side) and $^{197}_{79}\text{Au}_{118} + ^{197}_{79}\text{Au}_{118}$ (right side) at an incident energy of 50 MeV/nucleon

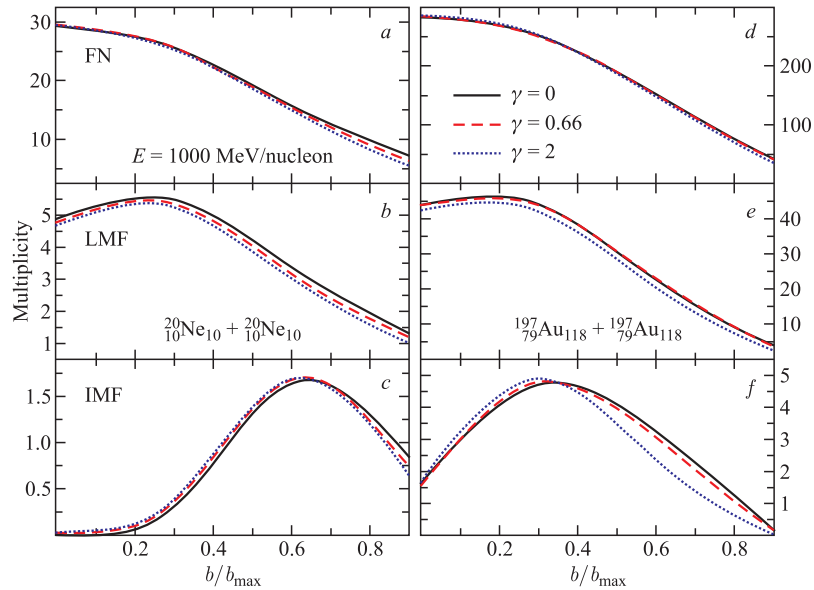


Fig. 4. Same as Fig.3 but at an incident energy of $E = 1000$ MeV/nucleon

In Fig. 3, we observed that the multiplicity of fragments (FNs, LMFs and IMFs) decreases with an increase in b/b_{\max} except for IMFs of $^{20}_{10}\text{Ne}_{10} + ^{20}_{10}\text{Ne}_{10}$ system. The reverse trend of IMFs in $^{20}_{10}\text{Ne}_{10} + ^{20}_{10}\text{Ne}_{10}$ system takes place because the colliding energy is unable to overcome the attractive force between the nucleons, so due to the large impact of mean field and attractive force between the protons due to the symmetry energy, the multiplicity of IMFs increases with increase in b/b_{\max} for neutron-deficient system. Moreover, one can see the effect of DDSE (soft or stiff) in neutron-deficient system more clear as compared to the neutron-rich system. In conclusion, we can say that the effect of DDSE decreases as one goes from neutron-deficient system to neutron-rich system in the low incident energy (attractive mean field) region.

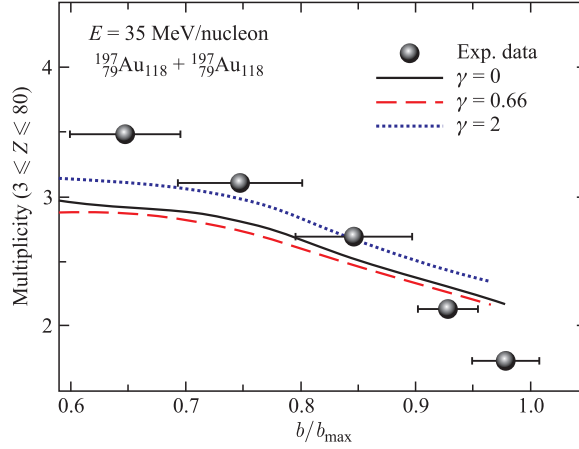


Fig. 5. A comparative study of theoretical calculations of IQMD with experimental data [15] of multiplicity of charged particles as a function of scaled impact parameter at $E = 35$ MeV/nucleon

In Fig. 4, the whole reaction mechanism is studied at high energy, i.e., $E = 1000$ MeV/nucleon. We observed that at high energy the multiplicity of fragments is almost independent of DDSE. This happened because at high energy the reaction dynamics depends only on NN collisions and it trims down the effect of DDSE on the multiplicity of fragments. To strengthen our results in Fig. 5, we display a comparative study of multiplicity of charged particles as a function of b/b_{\max} in the presence of momentum-dependent interactions. One can see that the theoretical calculated results with DDSE show the same trend as expected in experimental data. The disagreement in data can be overcome by using the experimental filters, which are not available with us. Le Fevre et al. [39] also deduced from data that the E_{sym}^0 for central collision is less as compared to the peripheral collision, so one can optimize the DDSE by changing the E_{sym}^0 .

CONCLUSION

Our study showed that the multiplicity of fragments depends on the incident energy. The density-dependent symmetry energy influences the fragment production at low energies (below 100 MeV/nucleon). The LMFs are found to be sensitive to the various forms of symmetry

energy as compared to FNs and heavier fragments for the whole range of incident energy. The effect of symmetry energy is larger in production of LMFs for neutron-deficient nuclei as compared to the neutron-rich nuclei.

Acknowledgements. This work has been supported by a grant from the Department of Atomic Energy (DAE), Government of India (Grant No. 2012/34/6/BRNS).

REFERENCES

1. Isospin Physics in Heavy Ion Collision at Intermediate Energies / Eds.: B. A. Li, W. Schroder. New York: Nova Science, 2011.
2. *Chen L. W., Ko C. M., Li B. A.* // Phys. Rev. C. 2007. V. 76. P. 054316.
3. *Li Z. H. et al.* // Phys. Rev. C. 2006. V. 74. P. 047304.
4. *Brown B. A.* // Phys. Rev. Lett. 2000. V. 85. P. 5296.
5. *Szmaglinski A., Wojcik W., Kutschera M.* // Acta Phys. Polon. B. 2006. V. 37. P. 227.
6. *Chen L. W., Ko C. M., Li B. A.* // Phys. Rev. C. 2005. V. 72. P. 064309.
7. *Zhao-Qing Feng* // Phys. Rev. C. 2011. V. 84. P. 024610.
8. *Chen L. W., Ko C. M., Li B. A.* // Phys. Rev. Lett. 2005. V. 94. P. 032701.
9. *Shetty D. V., Yennello S. J., Souliotis G. A.* // Phys. Rev. C. 2007. V. 75. P. 034602.
10. *Ma Yu-Gang et al.* // Phys. Rev. 2005. V. 69. P. 065610.
11. *Fang De-Qing et al.* // J. Phys. 2007. V. 34. P. 2173.
12. *Tian Went-Dong et al.* // Phys. Rev. C. 2007. V. 76. P. 024607.
13. *Shetty D. V., Yennello S. J., Souliotis G. A.* // Phys. Rev. C. 2007. V. 76. P. 024606.
14. *Shetty D. V. et al.* // Phys. Rev. C. 2005. V. 71. P. 024602.
15. *D'Agostino M. et al.* // Nucl. Phys. A. 1999. V. 650. P. 329.
16. *Hartnack C. et al.* // Eur. Phys. J. A. 1998. V. 1. P. 151.
17. *Jain A. et al.* // Phys. Rev. C. 2012. V. 85. P. 064608.
18. *Aichelin J.* // Phys. Rep. 1991. V. 202. P. 233.
19. *Lehmann E. et al.* // Phys. Rev. C. 1995. V. 51. P. 2113.
20. *Goyal S. et al.* // Nucl. Phys. A. 2011. V. 853. P. 164.
21. *Kumar S. et al.* // Phys. Rev. C. 1998. V. 58. P. 3494.
22. *Gautam S. et al.* // J. Phys. G. 2010. V. 37. P. 085102.
23. *Chugh R. et al.* // Phys. Rev. C. 2010. V. 82. P. 014603.
24. *Sood A. et al.* // Phys. Rev. C. 2006. V. 73. P. 067602.
25. *Puri R. K. et al.* // Phys. Rev. C. 1998. V. 57. P. 2744.
26. *Vermani Y. K., Puri R. K.* // Eur. Phys. Lett. 2009. V. 85. P. 062001.
27. *Vermani Y. et al.* // J. Phys. G: Nucl. Part. Phys. 2010. V. 37. P. 015105.
28. *Vermani Y. et al.* // J. Phys. G: Nucl. Part. Phys. 2009. V. 36. P. 105103.
29. *Puri R. K. et al.* // Phys. Rev. C. 1997. V. 45. P. 1837.
30. *Kumar S. et al.* // Phys. Rev. C. 1998. V. 58. P. 1618.
31. *Tsang M. B. et al.* // Phys. Rev. Lett. 2004. V. 92. P. 062701.

32. *Li B. A., Chen L. W.* // *Phys. Rev. C.* 2005. V. 72. P. 064611.
33. *Heiselberg H., Hjorth-Jensen M.* // *Phys. Rep.* 2000. V. 328. P. 237.
34. *van Dalen E. N. E., Fuchs C., Faessler A.* // *Nucl. Phys. A.* 2004. V. 744. P. 227.
35. *Piekarewicz J.* // *Proc. of the Intern. Conf. on Current Problems in Nuclear Physics and Atomic Energy.* V. 3. Kyiv, 2006.
36. *Famiano M. A. et al.* // *Phys. Rev. Lett.* 2006. V. 97. P. 052701.
37. *Danielewicz P.* arXiv:nucl-th/0411115.
38. *Schütauf A. et al.* // *Nucl. Phys. A.* 1996. V. 607. P. 457.
39. *Le Fevre A. et al.* // *Phys. Rev. Lett.* 2005. V. 94. P. 162701.

Received on December 13, 2012.